

WAD TR 52-43

DO NOT DESTROY

10

1657

RESEARCH CONTROL SECTION  
WCOSI-3

CATALOGED BY ASIA  
AS ATN No. 7504

# MEMORANDUM REPORT

ATI  
150 405

APPROVED FOR PUBLIC RELEASE-  
DISTRIBUTION UNLIMITED

AD A 075871

**U. S. AIR FORCE**  
**WRIGHT AIR DEVELOPMENT CENTER**

(Location)

20011214248

**SUBJECT:** Equations of Motion of the F-80 Aileron  
Boost

**SERIAL NUMBER:** WADC-52-43

**CLASSIFICATION:** None

**Reproduced From  
Best Available Copy**

**DATE:** March 1952

79 10 25 251

## NOTICES

When Government drawings, specifications, or other data are used for any purpose other than in connection with a definitely related Government procurement operation, the United States Government thereby incurs no responsibility nor any obligation whatsoever; and the fact that the Government may have formulated, furnished, or in any way supplied the said drawings, specifications, or other data, is not to be regarded by implication or otherwise as in any manner licensing the holder or any other person or corporation, or conveying any rights or permission to manufacture, use, or sell any patented invention that may in any way be related thereto.

The information furnished herewith is made available for study upon the understanding that the Government's proprietary interests in and relating thereto shall not be impaired. It is desired that the Office of the Judge Advocate (WCJ), Wright Air Development Center, Wright-Patterson AFB, Dayton, Ohio, be promptly notified of any apparent conflict between the Government's proprietary interests and those of others.

The U. S. Government is absolved from any litigation which may ensue from the contractor's infringing on the foreign patent rights which may be involved.

EQUATIONS OF MOTION OF THE F-80 AILERON BOOST

Samuel P. Altman, Captain, USAF

All-Weather Section  
Flight Test Division

United States Air Force  
Wright Air Development Center  
Wright-Patterson Air Force Base, Dayton, Ohio

EQUATIONS OF MOTION OF THE F-30 AILERON BOOST

Samuel P. Altman, Captain, USAF

United States Air Force  
Wright Air Development Center  
Wright-Patterson Air Force Base, Dayton, Ohio

## ABSTRACT

Equations and non-linear expressions defining the dynamic control performance of the F-80 aircraft aileron boost are derived. The complete equations and expressions define the non-linear nature of the device, and relate the instantaneous input and output moments to the input and output positions respectively, as determined by the boost design. Methods of solution by analogue machine methods are indicated for further investigation and study. These equations and expressions may be of use also in analysis of F-94 roll performance, since the boost design (with the exception of the hydraulic system pressure) is similar. The operation of the F-80 aileron differential mechanism is described as a related factor in the overall roll system control by a human pilot.

The security classification of the title of this report is UNCLASSIFIED.

## PUBLICATION REVIEW

Manuscript Copy of this report has been reviewed and found satisfactory for publication.

FOR THE COMMANDING GENERAL:



E. M. GAVIN, Colonel, USAF  
Chief, Flight Test Division

# TABLE OF CONTENTS

	<u>Page</u>
I - Introduction	
A. Purpose . . . . .	1
B. Description of Requirement . . . . .	2
II - Description of Boost Design Operation . . . . .	4
III - Analysis of the Boost Dynamics . . . . .	7
A. The Hydraulic Servosystem (Position) . . . . .	9
B. The Force Feedback System (Moment) . . . . .	12
IV - Resolution of Nonlinearity and Parameter Variation:	
A. The Hydraulic Servosystem . . . . .	13
B. The Force Feedback System . . . . .	14
V - Summation of Derivation and Suggested Machine Method for Solution . . . . .	18
VI - Design Function of the Aileron Differential Mechanism . . . . .	20
VII - Suggestions for Further Investigation . . . . .	21
Bibliography . . . . .	23
Appendix I - Feed-Thru Linkage Data Sheet . . . . .	33
Appendix II - Boost Valve Linkage Data Sheet . . . . .	34

# LIST OF ILLUSTRATIONS

<u>Figure</u>	<u>Description</u>	<u>Page</u>
1	F-30A Aileron Control System . . . . .	24
2-A, 2-B, 2-C	Boost Configuration . . . . .	25
3-A, 3-B	Functional Block Diagrams for Aileron Boost . . . . .	26
4	Kinematic Diagram of Feed-Thru Linkage . . . . .	27
5	Hydraulic Servosystem Characteristic (Output Velocity vs. Differential Displacement Error) . . . . .	28
6-A, 6-B	Effect of Input-Output Lag upon $\phi$ Transition . . . . .	29
7	Schematic Diagram for Proposed Machine Solution . . . . .	30
8	Schematic Diagram for Proposed Machine Solution (Including Effect of $R$ Gear Change on the A/C C/S Parameters) . . . . .	31
9-A, 9-B, 9-C	Effect of Aileron Differential Mechanism upon Hinge-Moment and Stick-Deflection Relations . . . . .	32

## I - INTRODUCTION

### A. Purpose

The development and presentation of the dynamic character of the F-80A aileron boost is set forth herein, in explicit analytical terms. No attempt has been made to side-step the basically nonlinear nature of the device. The proposition that the performance of this device is basically nonlinear is--aside from the contents of this report--substantiated by laboratory investigations reported in indicated references and by the use of the "aileron differential mechanism" in the aileron control system. The apparent usefulness of this differential device is briefly touched upon.

It is suggested that such a development and presentation may be of value in future development work on this class of device for the following reasons:

1. It assists in a clearer understanding of some outstanding factors influencing the dynamic performance of the complete aircraft control systems.
2. It provides an essentially historical record of the design development problems and the attendant difficulties, by implication.
3. It provides basic analytical data on a widely used and applied nonlinear device, for use in research into required techniques of nonlinear mechanics.

It should be noted that the final form of the mathematical statements is suited primarily for machine solution, rather than direct solution by classical mathematical techniques. This is done in recognition of the fact that analogue methods will be necessary for adequate solution and investigation. However, further treatment of the data and expressions--other than machine solution--could display many qualitative conclusions not readily apparent otherwise. It is hoped that associated workers in this field may find this development and presentation of sufficient interest and promise to warrant further investigation and use.

## B. Description of Requirement

The complete engineering problem was that of analysis of the problems and originating causes of unsatisfactory automatic control of the Type F-80A aircraft by the Type F-5 automatic pilot, about the roll axis. The special condition for concern was performance in the airspeed-altitude regime (and landing configuration) encountered in automatic approach and landing. This set of conditions is important for blind landing when radio signals are used from ILS, and coupled as inputs to the automatic pilot.

In general, instability phenomena of the following description were encountered:

1. At low altitude-airspeed combinations, a low-frequency, small-amplitude oscillation (about 0.5-0.75 degrees at 0.5-0.6 cps) was noted, in roll.
2. As the altitude and air speed are increased, a large-amplitude, low-frequency oscillation appeared; the amplitude increased as the altitude and air speed increased.

The above instability was evident in spite of adjustment of the automatic pilot calibration controls (displacement signal gain, rate signal gain and feedback signal gain) for optimum combinations.

The complete aircraft control system for control of roll motion (i.e., rotation about the aircraft longitudinal axis) is shown schematically in Figure 1. The human pilot can cause actuation of the ailerons (one on each wing) by side-wise motion of the control stick (2). Such motion causes rotation of the torque tube (3) which works through an "aileron differential mechanism" (4) to rotate the torque tube (11). The aileron differential mechanism is essentially a cam-type device which produces less angular rotation of torque tube (11) per degree of rotation of torque tube (3) about the neutral (or aerodynamic streamline) position of the control stick (2) than at other positions of the stick. As the stick is displaced from the neutral position, less stick motion is required to produce a given rotation of torque tube (11). Rotation of the torque tube (11) causes linear motion of the aileron control cables (7) through (and with the aid of) the aileron boost, (6). The linear motion of the control cable causes rotation of the aileron (9) about its hinge axis, through the use of the push-pull linkage (8) working from the aileron drum (10).

## B. Description of Requirement (contd)

The aileron boost serves two purposes, in this particular design:

1. To produce aileron drum rotation exactly (or as nearly as possible) equal to the torque tube (11) rotation, while -
2. Producing additional torque moment at the aileron drum in direct proportion to the input torque as measured at the torque tube (11).

Considerable opinion existed, to the effect that the instability phenomena encountered were due to boost dynamic performance, and also change of the aerodynamic derivatives (nondimensional coefficients in the aircraft equations of motion) with changes of air speed and altitude. However, the variables and parameters which affect the dynamic performance of the complete aircraft-automatic pilot system must be determined, together with the equations of motion which relate the variables and parameters functionally, in order that the phenomena may be identified with features of the physical design. Then the equations (and/or expressions) are used to identify the major causes of the instability phenomena through analysis and study, and to indicate possible redesign approaches or modifications.

The aircraft equations of motion and the automatic pilot components are available for use in the study of the complete system. Equations of motion (and/or mathematical expressions) for the boost dynamics were not available from other sources; consequently, it was necessary to derive equations of motion suitable for analytical study. The pertinent nonlinearities of design must be considered for the region implicitly defined by the instability phenomena. The use of the actual boost unit in a laboratory simulation of the system loop is not adequate, since the effects of many boost features are not readily apparent or predictable without an explicit mathematical statement. Therefore, the research problem reported here in greater engineering detail is that of derivation of the equations of motion (and/or mathematical expressions) defining the functional operation of the aircraft aileron boost control.

## II - DESCRIPTION OF BOOST DESIGN OPERATION

A physical schematic of the aileron boost is shown in Figure 2-A, 2-B, and 2-C. The input from the pilot's control stick to the boost system is introduced by rotation of the operating arm. The output to the aileron drum and aileron is introduced by linear motion of cables secured to the boost drum and riding in pulley grooves.

In order to observe and understand the general operation of the boost (prior to detailed analysis), let us first consider the boost configuration shown in Figure 2-A. Here, the operating arm is centered (and the pilot's control stick in neutral), while the aileron is streamlined. This configuration will be held as long as the control valve is positioned as shown; that is, link axis " $l$ " maintains the given position. (Note that the input control link has link axis " $j$ " located on the operating arm, while the output control link has link axis " $k$ " located on the boost drum. It can be seen that link axis " $l$ " can be re-positioned only if motion of the differential link occurs because of rotation of " $C_j$ " through an angle different from that of " $C_k$ ", since " $C_l k k$ " and " $j j' k' k$ " are similar parallelograms, at all times). With this boost configuration, the spring in the spring cartridge is not under load, and the pin fixed to the feel arm is located at the midpoint of the slot in the lower boost link. Also, the hydraulic system control valve is centered, so that pressure is locked in the hydraulic system on both faces of the actuating piston. Consequently, the piston and the actuating link are immovable until the pressure is somehow relieved.

Let us consider Figure 2-B. Here, the operating arm has just been rotated (or displaced) about center " $C_j$ " through a given angle " $\theta$ " while the aileron is still streamlined. As a result, motion of the differential link occurs so that the control valve is moved to the right. Hydraulic pressure is just building up on the right face of the actuating piston, while the fluid on the left face of the piston is being vented (or pressure relieved). The piston is on the verge of motion to the left. Meanwhile, the spring in the spring cartridge has been compressed as a result of rotation of the operating arm. At the same time, the boost drum is rotating about center " $C_j$ " while the actuating link axis " $e$ " is momentarily immovable.

## II - DESCRIPTION OF BOOST DESIGN OPERATION (contd)

Consequently, the feel arm rotates slightly about center " $C_2$ ", so that all effective mechanical elements are of compatible length and position. As a result of the rotation of the feel arm, the pin fixed to the feel arm moves in the lower boost link slot until it hits "bottom". From then on, the operating arm load is carried through the lower boost link rather than the spring cartridge link.

The boost configuration shown in Figure 2-C is obtained an extremely short time after that configuration shown in Figure 2-B. The actual time interval is dependent upon the response characteristics of the hydraulic system. (Note that the configurations shown in Figures 2-A and 2-C are in steady-state, or equilibrium condition, while the configuration shown in Figure 2-B is in a transient, or non-equilibrium condition). Here, (in Figure 2-C) the actuating piston has moved to the left, causing rotation of the boost drum about the center " $C_1$ " (with a small angle of rotation of the feel arm, back to its original position relative to the boost drum). The boost drum has been rotated until the output control link with center " $k$ " located on the boost drum has moved the differential link so that the control valve is once again positioned in its neutral (or center) position. Then, hydraulic pressure and relief ports are shut off from the cylinder, so that the actuating piston is held immovably in its new position. (In the actual case, fluid must be present on both faces of the piston; the schematic diagrams were simplified for explanation of the basic boost operation). In this configuration, the feel arm pin is almost restored to the midpoint position of the lower boost link slot. However, the spring cartridge is compressed, since the spring must be under load. This may be realized upon consideration of the presence of restoring moments on the aileron surface, expressed in terms of total hinge moment per unit of angular deflection. This term represents the (moment per degree of surface deflection from the streamline) resulting from airflow impinging on the surface (for the quasi-static rather than dynamic state). Once the boost (and consequently, the aileron) is displaced from neutral, a moment is required to hold the operating arm (and consequently, the boost drum) in the off-neutral position. As long as the feel arm pin is not "bottomed", the load is carried through the spring, thereby compressing it slightly. This means that the feel arm pin cannot be located at the true midpoint position of the lower boost link slot, because of the change in mechanical link length and position.

## II - DESCRIPTION OF BOOST DESIGN OPERATION (contd)

Clockwise rotation of the operating arm and the boost drum can be understood by reasoning analogous to that described above for counter-clockwise rotation. It need only be noted that the spring cartridge design dictates that the spring will be under load for both shortening or lengthening of the spring cartridge link.

### III - ANALYSIS OF THE BOOST DYNAMICS

The boost design will now be analyzed for explicit equations and parameters which will express its dynamic performance. Functional block diagrams will be used to assist in this process. The physical elements of the boost may be initially represented by the diagram shown in Figure 3-1. Here, input control variables are designated (or expressible) as input force ( $f_1$ ), applied at a moment arm to produce a moment ( $M_1$ ) acting through an angle of rotation ( $\phi_1$ ). The output control variables from the boost to the aileron drum are expressible as output force ( $f_2$ ), output moment ( $M_2$ ) and output angle of rotation ( $\phi_2$ ). By consideration of the boost operation as described, the following three operational objectives are seen as implicit in the design:

1. The output angle ( $\phi_2$ ) should be equal to the input angle ( $\phi_1$ ) at all times.
2. The output moment ( $M_2$ ) should be effectively increased--or "boosted" (essentially at a constant proportion)--relative to the input moment ( $M_1$ ). The ratio of output to input moment is usually defined as the "boost ratio".
3. The "boost ratio" (herein after designated by " $R$ ") should be smaller in the immediate region of neutral, and larger for large excursions from neutral.

For ideal operation, " $\phi_2$ " should always be maintained equal to " $\phi_1$ ", at every instant. Actually, lag in the hydraulic servo system will cause delivery of the boost moment (equal to  $M_2 - M_1$ ) to lag the instantaneous effective input moment " $M_1$ ", which is always acting on the control surface through the feed-through linkage. Note that the power required for the additional moment " $M_2 - M_1$ " is drawn from the boost hydraulic system upon controlled demand. A smaller input moment per degree of effort ( $M_1/\phi_1$ ) for a given aileron displacement is obtained around the neutral position when the spring cartridge link is the load-carrying member in the feed-through linkage. A large input moment per degree of effort is obtained when the lower boost link becomes the load-carrying member. At the instant that the change in the effective load-carrying link occurs, the boost ratio changes, while the total force carried in the link does not change. The boundary position of " $\phi_1$ " at which the change in boost ratio occurs, will be dependent primarily upon the control surface hinge moment per unit angular deflection.

### III - ANALYSIS OF THE BOOST DYNAMICS (contd)

(Actually, it is dependent, in complete theoretical terms, upon the complete dynamic characteristics of the aircraft control system). The larger the required input moment per degree of deflection ( $M/\phi$ ) the smaller will be the boundary value of the angular displacement (" $\phi$ ") from the neutral position.

The dynamic elements of the boost may be represented schematically as shown in Figure 3-2. All elements strictly of dynamic import to the hydraulic servosystem are enclosed in the dotted box. Box C represents the process function for control valve displacement ( $\Delta$ ) as a function of the difference ( $\phi_1 - B\phi_2$ ) between operating arm position ( $\phi_1$ ) and boost drum position ( $\phi_2$ ). Box B represents the relative amount of ( $\phi_2$ ) feedback to the process function Box C; that is, Box C is a pure differential, while Box B is a pure gain function. (Actually,  $B = 1$  for this given boost design, although another value might be selected, as necessary. The general case is considered, for purposes of analysis). Box D represents the process function for hydraulic fluid flow ( $Q$ ) as a function of control valve displacement ( $\Delta$ ). Box E represents the process function for boost drum angular velocity ( $\dot{\phi}_2$ ) as a function of hydraulic fluid flow ( $Q$ ). Since Box B represents positional feedback, the complete hydraulic servosystem control variable is a positional output; that is, although the boost drum velocity ( $\dot{\phi}_2$ ) is the explicit output, the boost drum position ( $\phi_2$ ) is controlled as a function of the operating arm position ( $\phi_1$ ). Box A represents the process function for output moment ( $M_2$ ) as a function of the input moment ( $M_1$ ). Note that the output moment ( $M_2$ ) is actually provided from two power sources--from the original moment supplied through the operating arm, and from the hydraulic power supply of the servosystem. Although it is desirable (theoretically) that the output moment ( $M_2$ ) should be a function of the input moment ( $M_1$ ) such that the output position ( $\phi_2$ ) would always be identical, instantaneously, to the input position ( $\phi_1$ ), servosystem lags inherent in the design prevent the realization of this ideal condition. Design nonlinearities stem, as secondary effects, from the influence of these lags upon the configuration of the feed-thru linkages of Box B.

### A. Hydraulic Servosystem (Position)

Let us first set up the transfer functions for the hydraulic servosystem for force ( $f_2/f_1$ ) and position ( $\phi_2/\phi_1$ ). These functions can be derived from study of the hydraulic servosystem. The transfer function for moment ( $M_2/M_1$ ) can be derived from a study of the feed-thru linkage (Box A). According to the notation instituted in the previous paragraph, the following expressions are obtained:

$$\Delta = C(\phi_1 - B\phi_2) \quad (1)$$

$$\text{and} \quad Q = D\Delta \quad (2)$$

$$\text{Therefore} \quad Q = DC(\phi_1 - B\phi_2)$$

(Note that D and C may not be interchanged unless it is known that their operational nature would not then be changed).

$$(3) \text{ Also, } \dot{\phi}_2 = EQ$$

$$\text{Therefore, } \dot{\phi}_2 = EDC(\phi_1 - B\phi_2)$$

Let us assume that

$$\phi_2 = k_2 f_2$$

$$\text{and} \quad \phi_1 = k_1 f_1$$

where  $k_2$  = Proportionality constant between  $\phi_2$  and  $f_2$ .  
 $k_1$  = Proportionality constant between  $\phi_1$  and  $f_1$ .

$$\text{Then} \quad \dot{\phi}_2 = \frac{d}{dt}(k_2 f_2) = k_2 \dot{f}_2 = EDC(k_1 f_1) - EDCB(k_2 f_2)$$

$$\text{Rearranging- } f_1 = \frac{k_2}{k_1 EDC} \dot{f}_2 + \frac{k_2}{k_1} \frac{EDCB}{EDC} f_2$$

(for the region defined where EDC does not become zero, for the values considered).

A. Hydraulic Servosystem (Position) (contd)

Then  $f_1 = a\dot{f}_2 + bf_2$

where  $a = \frac{k_2}{k_1 EDC}$

$$b = \frac{k_2 B}{k_1}$$

But

$$f_1 = as\dot{f}_2 + bf_2 = (as + b)f_2$$

where  $s$  = the complex transform variable.

$$\therefore \left(\frac{f_2}{f_1}\right) = \frac{1}{as + b}$$

$$\text{Or } \left(\frac{\phi_2}{\phi_1}\right) = \frac{k_2 f_2}{k_1 f_1} = \frac{k_2}{k_1} \left(\frac{f_2}{f_1}\right) = \frac{k_2}{k_1} \cdot \frac{1}{as + b}$$

The functions (or quantities) for  $a$ ,  $b$ ,  $k_2$  and  $k_1$  are determinate. Note that the preceding equations with the complex transform variable imply the assumption that initial conditions are zero.

# A. Hydraulic Servosystem (Position) (contd)

It should be noted that the assumption of Equations (4a) and (4b) implies that the inertia, damping and/or friction properties of the physical control system (from the boost drum to the aileron, and from the operating arm to the pilot's control stick) may be neglected, for purposes of this analysis. A more complete development of the transfer function for force ( $f_2/f_1$ ) would be of the following form:

$$\text{Let } \phi_2 = F_2(s) f_2$$

$$\text{and } \phi_1 = F_1(s) f_1$$

where  $F_2(s)$  = time-variant function relating  $\phi_2$  and  $f_2$  .

$F_1(s)$  = time-variant function relating  $\phi_1$  and  $f_1$  .

For a linear second-order system with constant coefficients--

$$F_2(s) = \frac{G_2}{I_2 s^2 + R_2 s + K''}$$

$$\text{and } F_1(s) = \frac{G_1}{I_1 s^2 + R_1 s + K'}$$

where  $G_2$ ,  $G_1$ ,  $I_2$ ,  $I_1$ ,  $R_2$ ,  $R_1$ ,  $K''$  and  $K'$  are apparent combined physical parameters effective relative to the operating arm and the boost drum.

$$\text{then } \dot{\phi}_2 = s\phi_2 = sF_2(s)f_2 = \text{EDC}[F_1(s)f_1 - BF_2(s)f_2]$$

$$\text{Or } [sF_2(s) + \text{EDCB}F_2(s)] f_2 = \text{EDCF}_1(s)f_1$$

Therefore--

$$\left(\frac{f_2}{f_1}\right) = \frac{\text{EDCF}_1(s)}{sF_2(s) - \text{EDCB}F_2(s)} = \frac{1}{\left[\frac{1}{\text{EDC}} \cdot \frac{sF_2(s)}{F_1(s)} + B \cdot \frac{F_2(s)}{F_1(s)}\right]}$$

## B. The Force Feedback System (Moment)

Let us consider the kinematic diagram of the feed-thru linkage, as shown in Figure 4, for development of the transfer function for moment ( $M_o/M_i$ ). Points  $C_1$ ,  $b$ ,  $e$ ,  $a$ , and  $C_2$  are axes of rotation for linkage members. Boost drum center " $C_1$ " and actuating link center " $e$ " are considered fixed relative to the linkage system, for kinematic analysis. (Note that the actuating link center " $e$ ", rather than the feel arm center " $C_2$ " must be the fixed member). Pertinent dimensions, angles and forces are defined as shown in the diagram. Assume that the input moment is " $M_i$ ", effective on link " $C$ " about center " $C_1$ ", and that the output moment is " $M_o$ ", effective on boost drum distance " $E$ " about center " $C_1$ ". Then

$$\begin{aligned} F_{bc_1} &= \frac{M_i}{C} \\ F_{ab} &= F_{bc_1} \cos \tau = \frac{M_i}{C} \cos \tau \\ F_{ae} &= F_{ab} \cos \beta = \frac{M_i}{C} \cos \tau \cos \beta \\ M_{ae} &= F_{ae} A = M_i \left( \frac{A}{C} \cos \tau \cos \beta \right) \\ F_{c_2e} &= \frac{M_{ae}}{G} = M_i \left( \frac{A}{CG} \cos \tau \cos \beta \right) \\ F_{c_2c_1} &= F_{c_2e} \cos \delta = M_i \left( \frac{A}{CG} \cos \tau \cos \beta \cos \delta \right) \\ M_o &= F_{c_2c_1} E = M_i \left( \frac{AE}{CG} \cos \tau \cos \beta \cos \delta \right) \\ \therefore \left( \frac{M_o}{M_i} \right) &= \frac{AE}{CG} \cos \tau \cos \beta \cos \delta = ER \end{aligned}$$

It can be seen from the above expression that the boost ratio (that is,  $ER = M_o/M_i$ ) is dependent upon the values for the effective link lengths  $A$ ,  $E$ ,  $C$ ,  $G$  and the angles for force resolution  $\tau$ ,  $\beta$  and  $\delta$ . However, lengths  $E$  and  $G$  remain constant under all conditions. From succeeding analysis, it was noted that the most profound influence upon the boost ratio was due to changes in lengths  $A$  and  $C$ . Although angles  $\tau$ ,  $\beta$  and  $\delta$  do affect the boost ratio at all times, the influence of these angles is secondary, relative to that of the lengths  $A$  and  $C$ .

#### IV - RESOLUTION OF NONLINEARITY AND PARAMETER VARIATION

The presentation to this point is now complete in outline of the basic nature of the boost design details. At this time, it is advisable to reexamine the complete analysis made thus far, in order to determine the additional data and analytical techniques required to obtain the final statements for the boost dynamic performance. Upon consideration of the available data, it was deemed advisable to develop expressions most suitable for machine solution, rather than the formal equations such as Equations (5) and (6). Although this form of development could be carried to its logical conclusion, solution would not be simple--if possible at all. Machine solution offers promise for solution of engineering utility, with a reasonable number of manhours.

##### A. The Hydraulic Servosystem

Essentially, the transfer characteristics for Boxes B, C, D, E, and A must be determined. For this given boost design,  $B = 1$ , although other values within a finite and determinate range are physically realizable, with little or no effect upon the transfer characteristics of the other boxes. The transfer characteristics of Box C may be closely approximated by the following expression (derived from the valve linkage configuration):

$$\Delta = 0.037 (\phi_1 - \phi_2)$$

where  $\Delta$  = control valve displacement (in inches)

$(\phi_1 - \phi_2)$  = angular difference between input and output (in degrees)

Experimental data are required for determination of the transfer characteristics for Boxes D and E, unless extensive design data on and theoretical knowledge of the hydraulics of the servosystem are known. Such data are available from the following reference sources:

AF Technical Report No. 5977, titled "Investigation of F-80 Aileron Boost", dated March 1950.

Sperry Gyroscope Co. Report 5232-3118, titled "Frequency Response Investigation of an F-80 Aileron Booster", dated January 26, 1950.

#### A. The Hydraulic Servosystem (contd)

The required data, plotted as  $\dot{\phi}_2$  (in degrees/second) versus  $\Delta$  (in inches) or (in degrees) are shown in Figure 5. It can be seen that both curves might be considered as cubical parabolae, up to  $\Delta \approx 0.074"$ . The curve extracted from the AF Technical Report data was used, since the experimental technique used to obtain it was described in the report; while the limitations of this experimental technique can be appreciated, the technique used to obtain the Sperry curve is unknown. The desired expression is then

$$[\dot{\phi}_2]^2 = 4 \times 10^6 [\Delta]^3$$

where  $\Delta$  = control valve displacement (in inches)  
 $\dot{\phi}_2$  = angular velocity of output (in degrees/second)

The complete transfer characteristics for Boxes C, D, and E may be expressed as follows:

$$[\dot{\phi}_2]^2 = 202.6 [\phi_1 - \phi_2]^3$$

This expression is really a combination of Equations 8 and 9. However, it may be more desirable here, for machine solution, than the two individual expressions.

#### B. The Force Feedback System

The transfer characteristic for Box A is somewhat more complex, as a result of the unusual mechanical configuration. Upon studying the configuration, it becomes evident that two operating conditions occur simultaneously, to determine the boost ratio effective at any given instant of time:

1. Compression of the spring in the spring cartridge link, as the boost drum is rotated.
2. Change in the linkage configuration with lag in positioning the boost drum ( $\phi_2$ ) relative to the position of the operating arm ( $\phi_1$ ).

## B. The Force Feedback System (contd)

It may be recalled from the general description, that the position of aileron angular displacement from neutral position at which a change in boost ratio (caused primarily by a change in lengths A and C) occurs, is dependent upon the aileron surface load per degree of deflection from a streamline (or trim) position. This change is due to compression of the spring and consequent shortening (or lengthening) of the spring cartridge length, when such aileron moments arise. The lower boost link becomes the load-carrying member as the pin on the feel arm bottoms (or tops) in the slot, since the configuration changes with changes in linkage lengths. The greater the aileron moment per degree of aileron deflection, the smaller will be the aileron deflection from the neutral position, at which boost ratio change occurs. This operating condition, for purposes of analysis, is negligible, since the largest aileron deflection for boost ratio change (encountered at touch-down) is but a small fraction of a degree (less than 0.025 of a degree).

The other condition encountered may be appreciated by consideration of the linkage configuration, as shown in Figure 4. If the operating arm is deflected through a given angle, and the hydraulic servosystem lags (in time) in repositioning the boost drum to that angle, then an angular difference (in space degrees) will exist at a given instant. That is, presence of lag (in space degrees difference in angular position) caused by inability of the hydraulic servosystem to exactly match " $\phi_2$ " with " $\phi_1$ " at any instant of time, will cause different values of  $\dot{A}$ ,  $C$ ,  $\tau$ ,  $\beta$  and  $\delta$  than would occur with ideal servosystem performance. The angle " $\epsilon$ " will be changed in the kinematic diagram by the amount of that angular difference (in space degrees).\*\* This change in linkage configuration will primarily affect

- a. The boost ratio values encountered and,
- b. The displacement at which boost ratio value changes abruptly (when slot pin "bottoms" or "tops").

\*\* The change in angle " $\epsilon$ " should not be confused with the aileron deflection for boost ratio change described in the preceding paragraph. The change in angle " $\epsilon$ " (as shown in Figure 6-B) is the sum of the aileron deflection noted above, and operating arm deflection. Since the aileron deflection (for extreme case) will not exceed about 0.025 of a degree, it is assumed that all change in angle " $\epsilon$ " will occur in the operating arm deflection.

## B. The Force Feedback System (contd)

The following table lists the boost ratio values, as obtained from kinematic layout for lag (in space degrees) shown:

<u>Lag in Space Degrees</u>	<u>R in Neutral</u>	<u>R in Low Boost (CW)</u>	<u>R in High Boost (CW)</u>	<u>R in Low Boost (CCW)</u>	<u>R in High Boost (CCW)</u>
0	2.217	2.006	12.663	2.393	12.949
1/2	2.217	2.050	12.727	2.282	12.907
1/2	2.217	2.110	12.752	2.245	12.934
1-1/2	2.217	2.149	12.802	2.195	12.930
2	2.217	2.219	12.815	2.138	12.906
2-1/2	2.217	2.250	12.854	2.095	12.923
3	2.217	2.324	12.810	---	---
Max.% deviation from $R_0$	- - -	15.85	1.16	12.45	0.33

It is considered satisfactory to assume that

$$R_{Low} = R_{Neutral} = 2.25$$

$$R_{High} = 12.85$$

The position of abrupt ratio transition (that is, change from a nominal value of 2.25 to a nominal value of 12.85) varies with the lag between input and output. If the variation in the linkage configuration did not affect the position of boost ratio transition, the curve for  $\phi$  transition vs.  $(\phi_1 - \phi_2)$  would consist of the dotted straight lines in Figure 6-B, for lags up to 3 space degrees clockwise rotation or 2.7 space degrees counter-clockwise rotation. For lags greater than 3 or 2.7 space degrees (as applicable),  $\phi$  transition is then constant. However, for lags up to 3 or 2.7 space degrees (as applicable) the variation in linkage configuration requires an additional angle of rotation for before the position for boost transition occurs. The change in this required increment in  $\phi$  transition with  $(\phi_1 - \phi_2)$  is plotted in Figure 6-A. Consequently, the actual curve for  $\phi$  transition vs.  $(\phi_1 - \phi_2)$  is shown in solid lines in Figure 6-B. This curve is obtained by adding the increment of  $\phi$  transition to the value of input-output lag; that is,

$$\phi \text{ transition} = (\phi_1 - \phi_2) + \Delta\phi \text{ transition}$$

B. The Force Feedback System (contd)

This curve shows graphically that an effective lag (or dead-spot) in boost ratio change occurs at all times, even for zero lag. Although simplification of this curve may be warranted with suitable assumptions for ease of solution, this step will not be attempted in this report.

## V - SUMMATION OF ANALYSIS AND SUGGESTED MACHINE METHOD FOR SOLUTION

The data and mathematical expressions defining the dynamic performance of the F-80A aileron boost are now complete. Equation (10), together with Figure 6-B may be considered as a complete compilation of the necessary information (together with the process diagram relating the given variables), although any of the other equations may be used as branchpoints for analysis. At the same time, the following summarized assumptions and notes are applicable:

1. The effect of control inertia and damping was considered negligible for the evolution of Equations (5) and (6).

2. The effects of hydraulic pressure and fluid volume flow are not explicitly related to the dynamic performance in these expressions.

3. The effect of values of "B" other than unity are not here considered.

4. Equation (8) may be considered valid only up to absolute values of  $(\phi_1 - \phi_2) = 2^\circ$  (or  $\Delta = 0.074$ ). \*

As noted previously, solution for the defined performance is most feasible (for this laboratory) by the use of analogue machine methods. A schematic diagram for proposed machine solution is shown in Figure 7. Input quantities are  $\phi_1$  and  $M_1$ . Operations 1, 2, and 4 may be accomplished by linear electronic analogue computer channels. Operation 3 may be achieved by a nonlinear electronic (or electromechanical) analogue computer network. Operation 5 may be obtained by a nonlinear analogue network, automatic tracking plotting table or follower with good response characteristics. A gating or relay contactor type device could be used for Operation 6. The required outputs would be  $\phi_2$  and  $M_2$ .

---

\* If the input-output lag for a given problem should exceed two spaces degrees, then a more satisfactory equation will be needed. However, it is felt that only the most unusual problems will require such consideration.

## V - SUMMATION OF ANALYSIS AND SUGGESTED MACHINE METHOD FOR SOLUTION (contd)

The input quantities may be derived from computer networks or from a servosystem with physical characteristics (or parameters) such that a desirable relation of  $M_1$  and  $\phi_1$  may be obtained; that is, so that the transfer functions for  $(M_2/M_1)$  and  $(\phi_2/\phi_1)$  are most desirable for the given application. It is recognized that this procedure falls within the realm of synthesis, rather than analysis and investigation of an existent system.

Further data on control system inertia and damping will be necessary, for analysis of the given F-80 aircraft control system. The necessity for these data can best be realized by consideration of Figure 8. Here, a schematic diagram for proposed machine solution has been set up, in order to relate  $\phi_1$  (as the dependent variable) to  $M_1$  (as the independent variable). Both the control system parameters on the input side of the boost, and the control system parameters on the output side of the boost are defined by the function  $F_1(s)$ . The control quantity " $v_y$ " is fed into a multiplier to account for the change in apparent effective value of c/s parameters on the output side, as seen at the input side; that is, a change in gear ratio must be made. Such aircraft control system data may be obtained from aircraft manufacturer's engineering reports, and/or study reports by interested research groups.

Note that  $F_1(s)$  and  $F_2(s)$  defined on Page 10 are different expressions relating the same parameters. One implication may be drawn from this condition: namely, that the variables  $M_2$  and  $\phi_2$  are not truly independent, as might be erroneously concluded by cursory examination of the schematic diagram in Figure 8. Actually, the situation might be better clarified by considering the transfer function of the boost in terms of power. The output power defined by  $(f_2; \phi_2; M_2)$  is greater than the input power defined by  $(f_1; \phi_1; M_1)$ . The difference is supplied by the hydraulic power supply. The boost should most accurately be visualized as a power control device, rather than a positional or moment control device. Machine solution in accordance with the schematic diagram in Figure 8 should reveal the time-variant characteristics of the power demand upon the hydraulic power supply.

## VI - DESIGN FUNCTION OF THE AILERON DIFFERENTIAL MECHANISM

The design operation of the aileron differential mechanism was described briefly in the introduction, and is shown in the control system diagram of Figure 1. The function of this device deserves a little discussion in this report, since it is somewhat related to the nonlinearities inherent in the boost design.

The differential mechanism will provide more stick rotation per unit aileron deflection at neutral than at out-of-neutral positions, as shown in Figure 7A. This means that, for a given constant hinge-moment per unit deflection, less force is needed about neutral to cause a unit stick rotation. Or, for example, suppose that the hinge moment ( $HM_a$ ) vs. aileron deflection ( $\delta_a$ ) curve is as shown in Figure 7B, and the boost performance is ideal. Then this curve can also be considered as representing the input moment ( $M_i$ ) vs. input boost position ( $\phi_i$ ) curve. Then the relation for stick moment per unit stick rotation vs. aileron deflection may be found by super-imposing the curve of Figure 9-A upon the curve of Figure 9-B, and dividing the curve value for  $HM_a$  (or  $\phi_i$ ) by the corresponding value for  $\phi$  stick at each  $\delta_a$  (or  $\phi_i$ ) value. For example, at aileron value  $\delta_a = a$  (abscissa value), divide  $HM_a = b$  (ordinate value) by  $\phi_{stick} = c$  (ordinate value). Then curve D of Figure 9-C will be obtained. Curve E of Figure 9-C shows the relation obtained for a constant ratio of  $\phi$  stick to  $\phi_i$ ; that is, for  $\phi_{stick} = K\phi_i$ . It can be seen that a greater ( $M_{stick} / \phi_{stick}$ ) is obtained (up to  $\delta_{a0}$ ) by use of the differential mechanism. So-called "feel", used by the human pilot for control, is proportional primarily to this ( $M_{stick} / \phi_{stick}$ ). Consequently, the pilot is given greater "feel" over this range.

This greater "feel" will help slightly to minimize the effect of variable boost ratio, for boost response giving space degrees phase lag of the order shown in Figure 6-B. However, it will be detrimental in obtaining satisfactory stability, in the presence of significant Coulomb-type friction or dead-spot; that is, if the stick movement (or roll rate) required is small, then a human pilot may be unable to hold the aircraft in a given roll attitude, without a certain amount of oscillation.

## VII - SUGGESTIONS FOR FURTHER INVESTIGATION

Although solution of the previously derived expressions is most desirable for an adequate understanding of the dynamic characteristics of the boost design, it is nevertheless possible to obtain qualitative significance from these expressions, by examination. In general, at lower " $q$ " values (when lower hinge moment coefficients occur), the nonlinear relation of  $\phi$  vs.  $\Delta$  is significant while the change in boost ratio should be negligible in its effect on dynamic performance. At higher " $q$ " values (when higher hinge moment coefficients occur), the change in boost ratio can- and in most cases does-become significant. That is, whenever hydraulic servosystem phase lag of any significant amount is present, then the change in boost ratio must be considered. Such servosystem lags will occur whenever higher rates of stick motion are required; the actual order of magnitude of these rates can only be obtained either from more complete analysis, or flight test data. It is suggested that the variable boost ratio design element is required to overcome effects such as Coulomb-type friction; however, this may only be confirmed by laboratory investigation.

It should be noted that while the hydraulic servosystem response is largely dependent upon the relation of  $\phi$  vs.  $\Delta$  and essentially independent of load moment, the feed-thru linkage effects a change in boost ratio (or "load moment gain") as a function of the hydraulic servosystem response and the hinge-moment per degree angular deflection. As a consequence, the overall boost response is rather complex, and requires more detailed analysis for a clearer understanding of its design. Such devices as this boost may be better analyzed and understood by application of the concept of time-variant control of the power. It is believed by the author that such an approach offers the greatest promise for rational interpretation of the significant performance characteristics of such basically nonlinear servomechanical devices and/or systems.

It is suggested that laboratory tests for significant dynamic parameters of the hydraulic servosystem (such as Coulomb-type friction, deadspot and effects of hydraulic pressure drop) might provide a still clearer understanding of the dynamic characteristics. Also, investigation into the relative performance of this boost design compared with the performance of the F-94 boost design should reveal interesting differences. The primary difference between these boosts is that the

## VII - SUGGESTIONS FOR FURTHER INVESTIGATION (contd)

F-80 and F-94A boosts are designed for 1000 psi. hydraulic pressure, while the F-94B and F-94C boosts are designed for 1500 psi. hydraulic pressure. In all other respects, the designs are almost identical. Redesign for increased hydraulic pressure stems apparently from a need for improved boost performance, since the F-80 and F-94 aircraft response characteristics are quite similar for the lateral modes of motion.

## BIBLIOGRAPHY

Air Force Technical Report No. 5977, Investigation of F-80 Aileron Boost, March 1950

Sperry Gyroscope Co. Report 5232-3118, Frequency Response Investigation of an F-80 Aileron Booster, January 26, 1950.

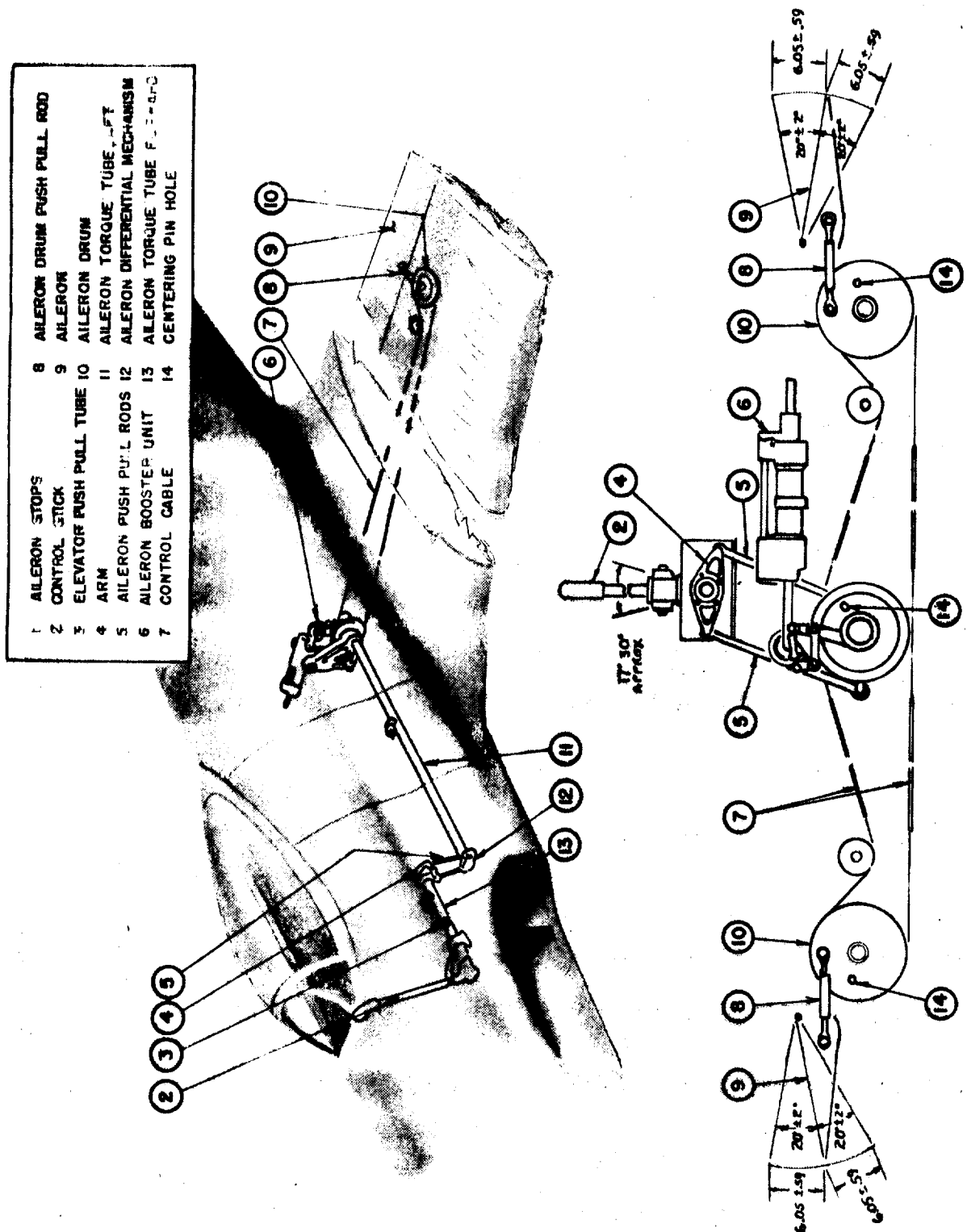


FIGURE 1 F-80A AILERON CONTROL SYSTEM

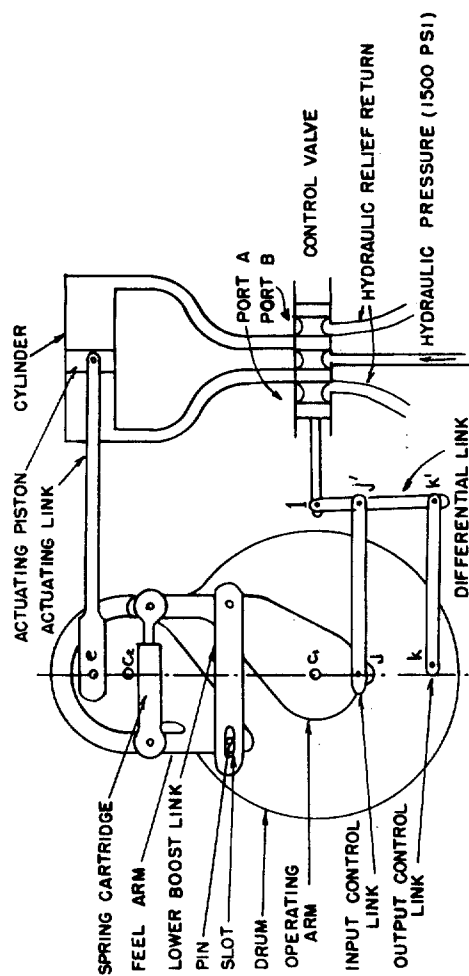


FIGURE 2-A BOOST CONFIGURATION FOR {AILERON STREAMLINED  
OPERATING ARM CENTERED

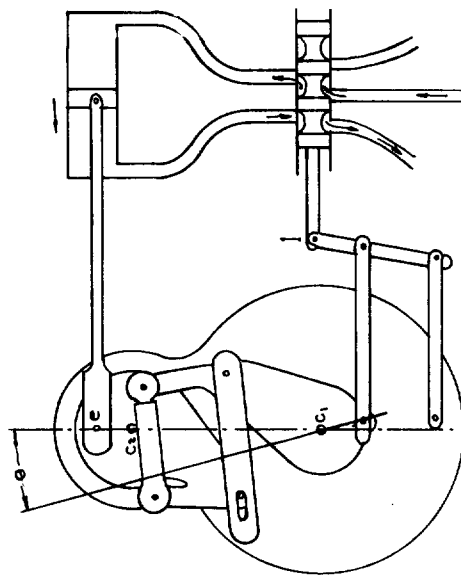


FIGURE 2-B BOOST CONFIGURATION FOR {AILERON STREAMLINED  
OPERATING ARM DISPLACED

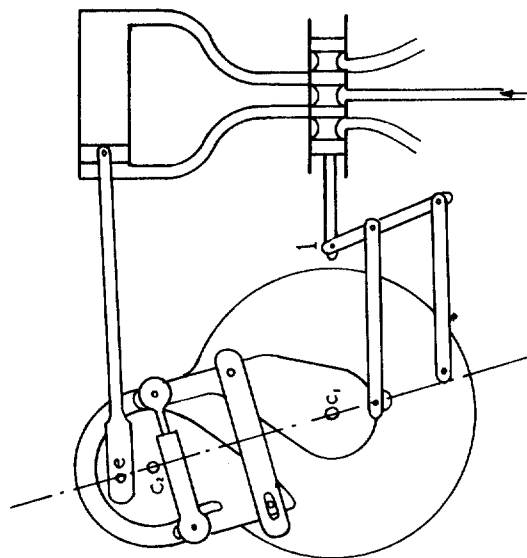


FIGURE 2-C BOOST CONFIGURATION FOR {AILERON DISPLACED  
OPERATING ARM DISPLACED

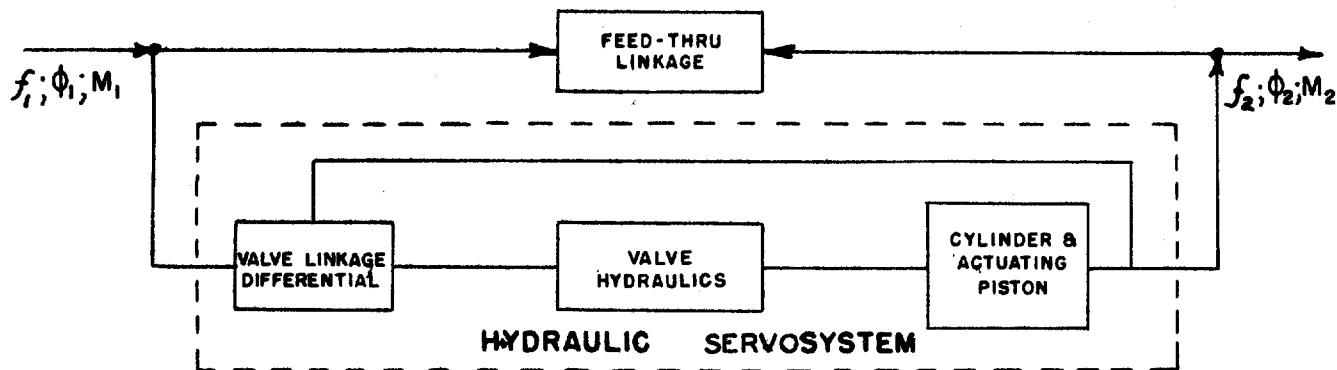


FIGURE 3-A FUNCTIONAL BLOCK DIAGRAM OF  
PHYSICAL COMPONENTS OF AILERON BOOST

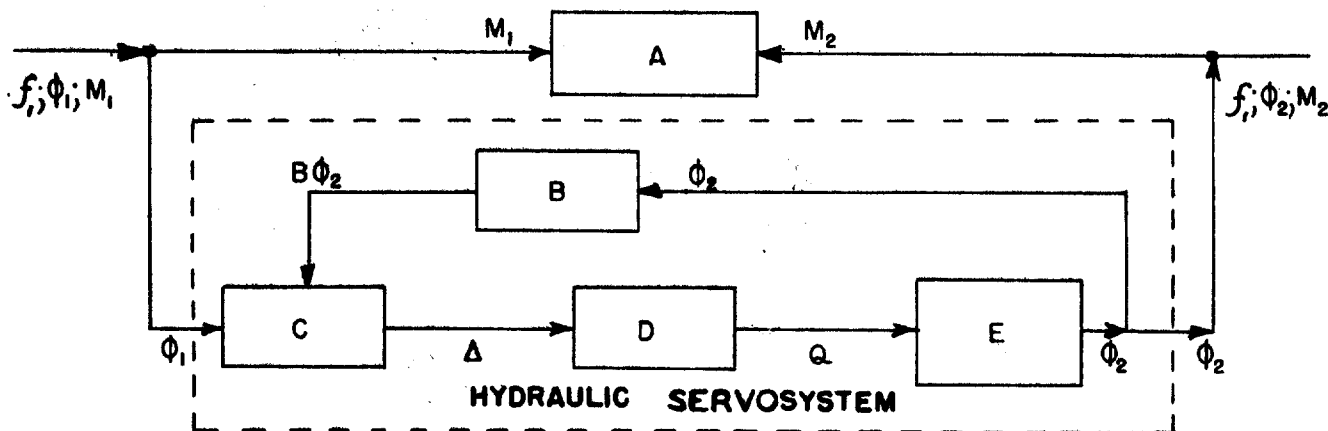


FIGURE 3-B FUNCTIONAL BLOCK DIAGRAM OF  
DYNAMIC ELEMENTS OF AILERON BOOST

$M_1$  = input moment.

$f_1$  = input force caused by input moment, effective at given input reference point.

$\phi_1$  = angular deflection of input reference point resulting from input moment.

$M_2$  = output moment.

$f_2$  = output force caused by output moment, effective at given output reference point

$\phi_2$  = angular deflection of output reference point, resulting from output moment.

A = transfer function for  $(M_2/M_1)$

B = amount of  $\phi_2$  feedback, relative to  $\phi_1$  (i.e. expressed as a percentage of  $\phi_1$ )

C =  $(\phi_1 - B\phi_2)$ , i.e., a differential process.

D = transfer function for  $(Q/\Delta)$ .

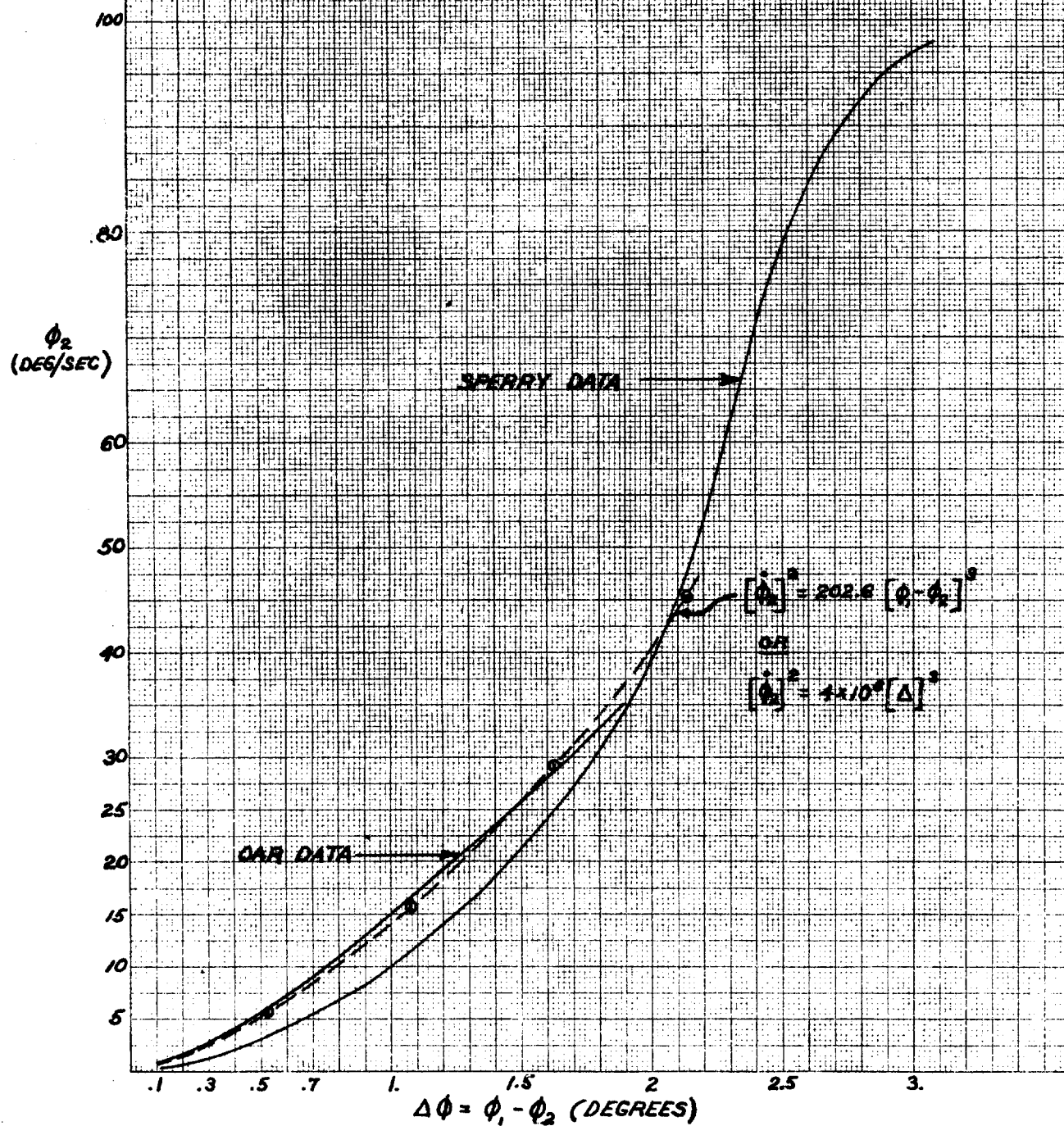
E = transfer function for  $(\phi_2/Q)$ .

$\Delta$  = control valve displacement.

Q = volume of hydraulic fluid flow.



**FIGURE 5 HYDRAULIC SERVOSYSTEM CHARACTERISTIC  
(OUTPUT VELOCITY VS DIFFERENTIAL  
DISPLACEMENT ERROR)**



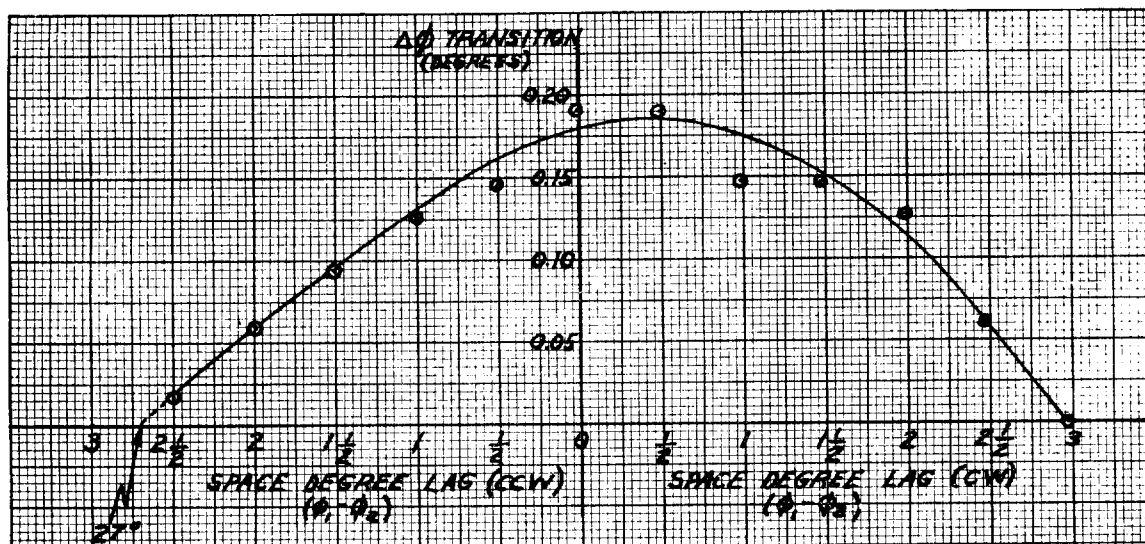


**FIGURE 6-A** EFFECT OF INPUT-OUTPUT LAG UPON INCREMENT OF  $\phi_{\text{TRANSITION}}$  DUE TO LINKAGE CONFIGURATION

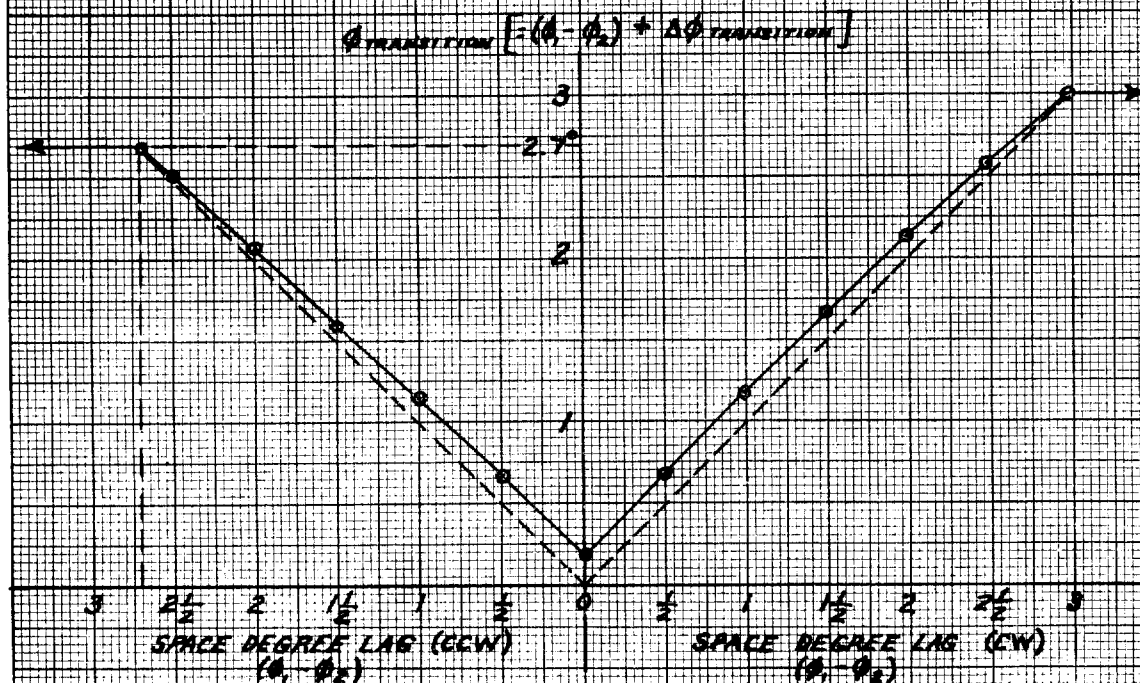


**FIGURE 6-B**  $\phi_{\text{TRANSITION}}$  VS INPUT-OUTPUT LAG

**NOTE:**  $\phi_{\text{TRANSITION}} = (\phi_1 - \phi_2) + \Delta\phi_{\text{TRANSITION}}$ ; i.e., VALUE OF  $\phi_1$  FOR THE GIVEN INSTANT WHEN  $\phi_2$  CHANGES.  $\phi_1 < \phi_{\text{TRANSITION}}$  GIVES LOW BOOST, WHILE  $\phi_1 > \phi_{\text{TRANSITION}}$  GIVES HIGH BOOST.

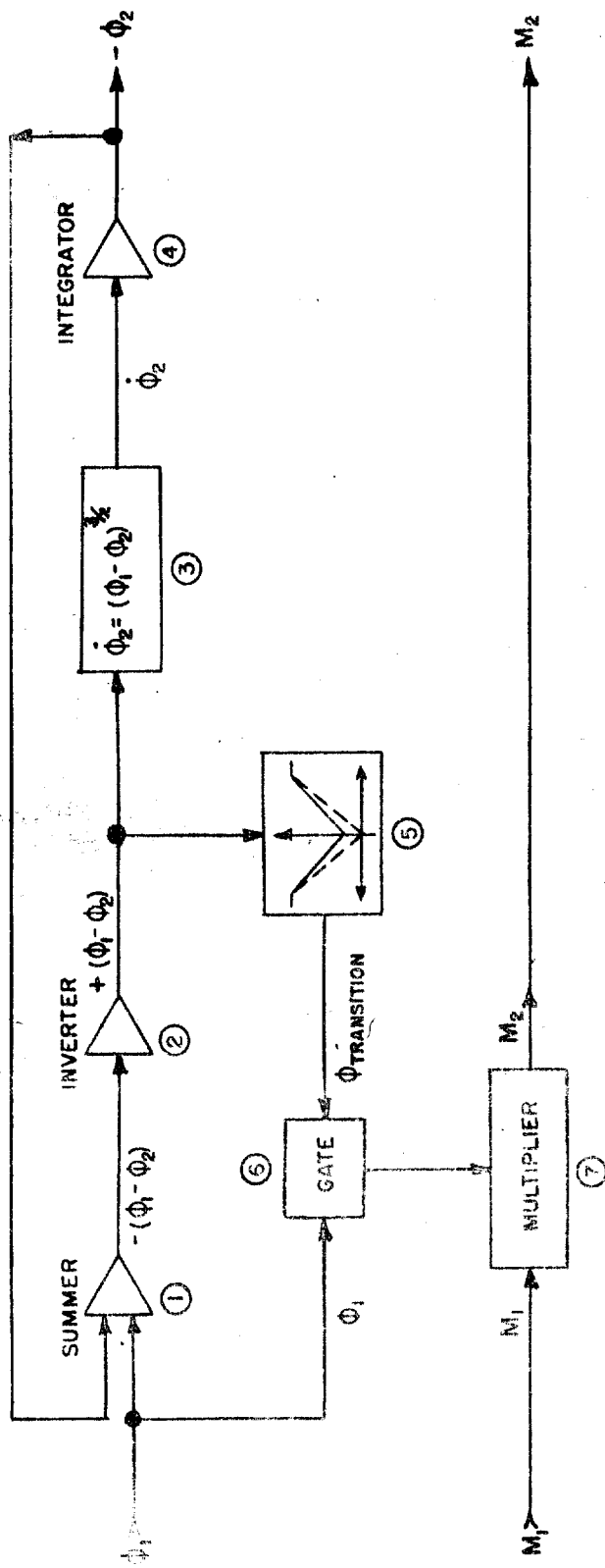
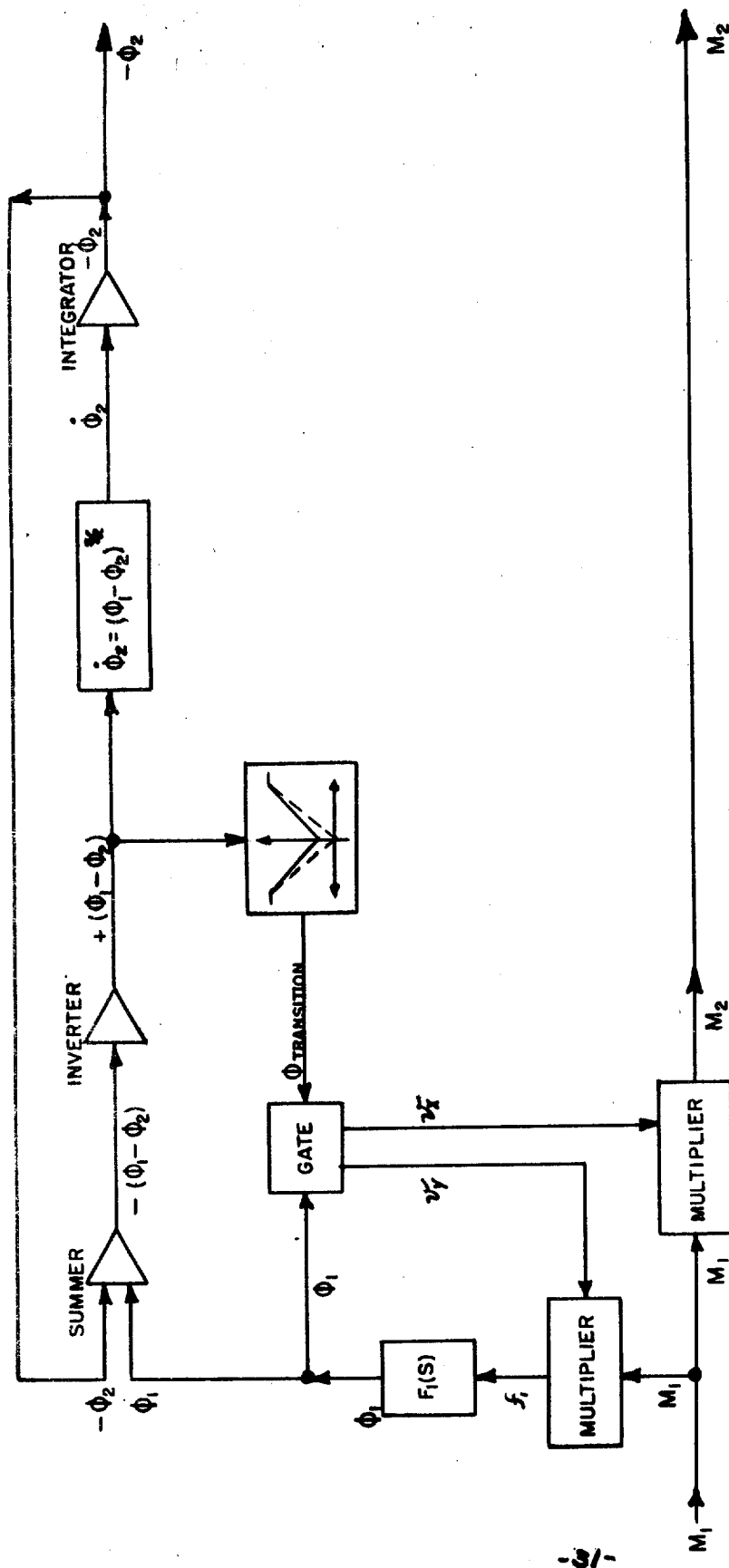


FIGURE 7 SCHEMATIC DIAGRAM FOR PROPOSED MACHINE SOLUTION

NOTE:  $\begin{cases} v' = v_1 & \text{WHEN } \phi_1 < \phi_{\text{TRANSITION}} \\ v' = v_2 & \text{WHEN } \phi_1 > \phi_{\text{TRANSITION}} \end{cases}$   
OR  
 $\begin{cases} v' \propto R_{\text{LOW}} \\ v' \propto R_{\text{HIGH}} \end{cases}$



**FIGURE 8** SCHEMATIC DIAGRAM FOR PROPOSED MACHINE SOLUTION (INCLUDING EFFECT OF  $\phi$  GEAR CHANGE ON THE A/C C/S PARAMETERS)

NOTE:

$v_X = v_{X1}$	} WHEN $\phi_1 < \phi_{\text{TRANSITION}}$
$v_Y = v_{Y1}$	
$v_X = v_{X2}$	} WHEN $\phi_1 > \phi_{\text{TRANSITION}}$
$v_Y = v_{Y2}$	

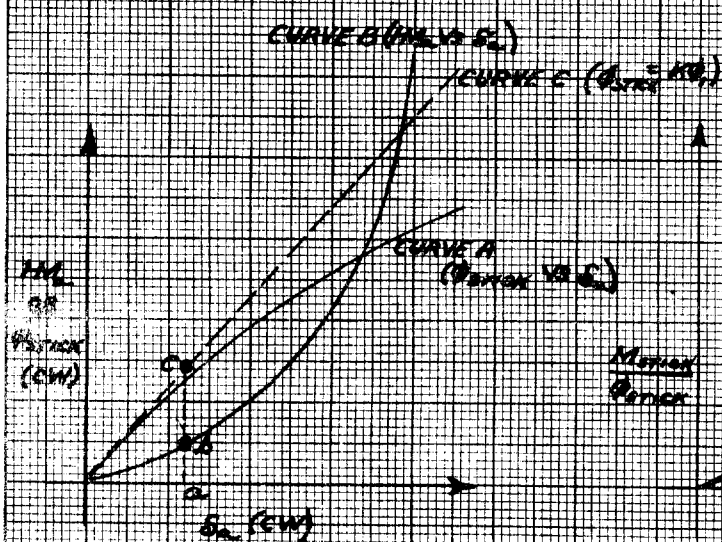
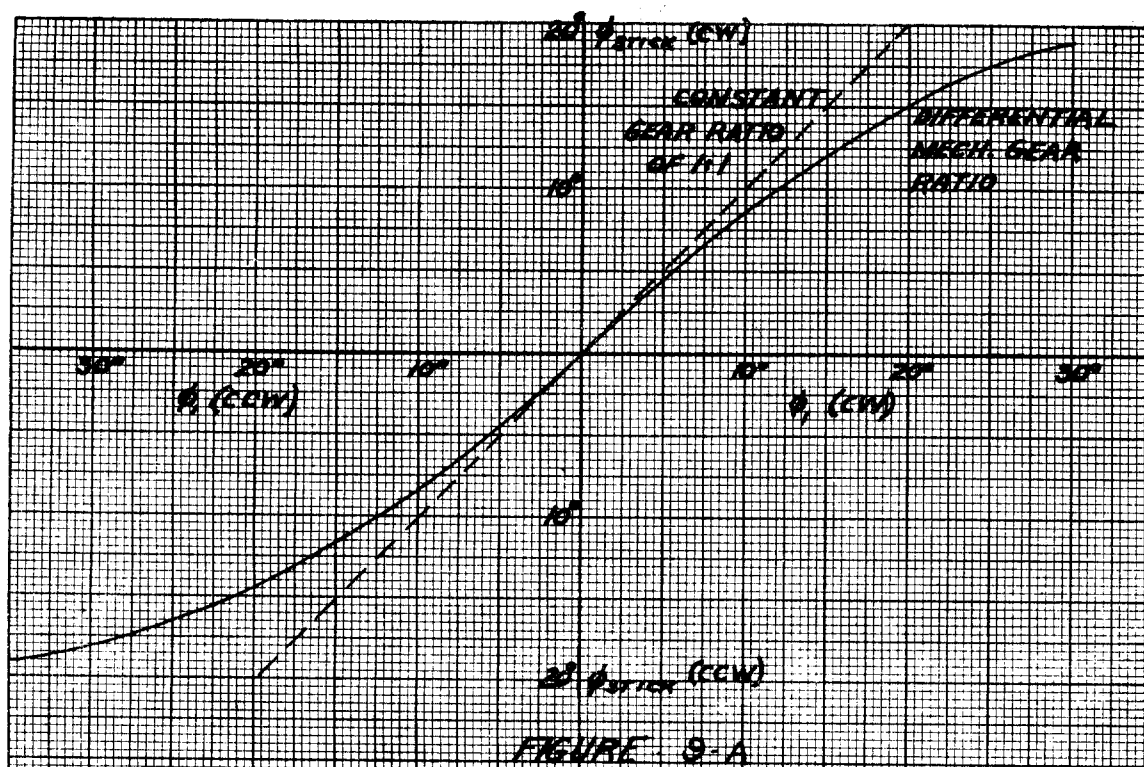


FIGURE 9-B

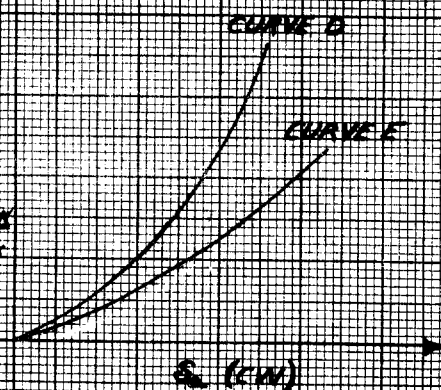
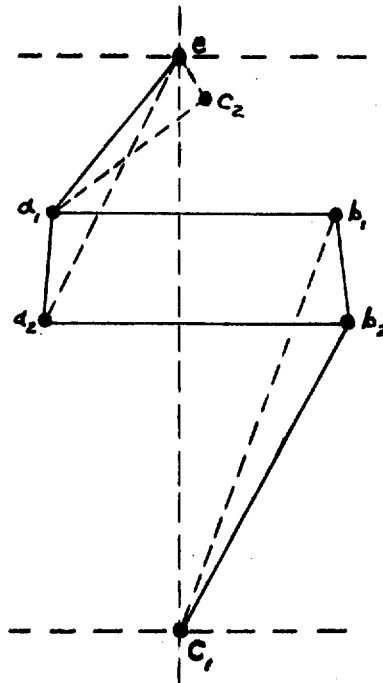


FIGURE 9-C

(NOTE: THE RELATION FOR IM vs  $S_{\text{IN}}$  IS NOT BASED ON A GIVEN SET OF DATA, BUT IS ILLUSTRATIVE ONLY)

# **APPENDIX I** **FEED-THRU LINKAGE DATA SHEET**

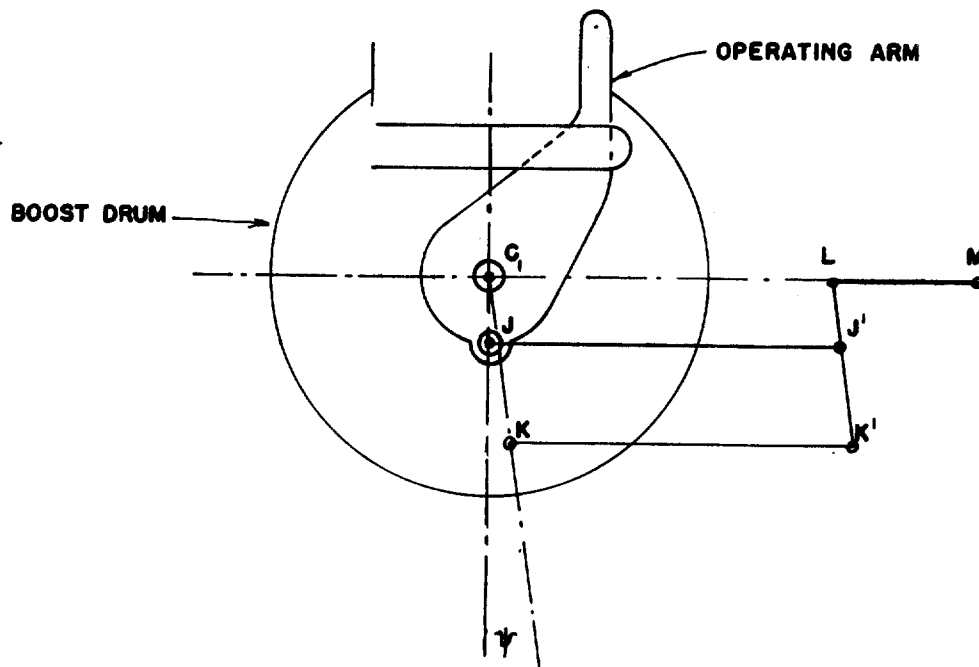


$e c_1 = 6.227"$   
 $c_1 b_2 = 3.8748"$   
 $c_1 b_1 = 5.929"$   
 $b_2 b_1 = 2.281"$   
 $a_2 a_1 = 1.900"$   
 $e a_1 = 1.9917"$   
 $e a_2 = 3.2093"$   
 $e c_2 = 0.290"$   
 $a_1 c_2 = 1.9219"$

$a_1 b_1$  (neutral) = 4.000"  
 $a_1 b_1$  (minimum) = 3.45"  
 $a_1 b_1$  (maximum) = 4.56"  
 $a_2 b_2$  (neutral) = 4.031"  
 $a_2 b_2$  (minimum) = 3.8435"  
 $a_2 b_2$  (maximum) = 4.2185"

spring rate for  $a_1 b_1$  deflection = 11 lbs. per in.

APPENDIX II  
BOOST VALVE LINKAGE DATA SHEET



$GK = 3.000''$   
 $GJ = 1.250''$   
 $JJ' = 4.875''$   
 $KK' = 4.875''$   
 $K'J' = 1.75''$   
 $K'L = 3.00''$   
 $LM = 1.28''$   
 $\psi = 7^{\circ}44'$

DISTRIBUTION:	<u>No. of Copies</u>		<u>No. of Copies</u>
Director of Operations, Hq USAF Washington 25, D. C.	(2)	WCR Research Division, Hq WADC, WPAFB	(1)
Lt. Colonel T. F. Walkowicz, AFCCS-SA, Room 5 E 1015, Hq USAF Washington 25, D.C.	(2)	WCTA Administration Office, Flight Test Division, Hq WADC, WPAFB	(1)
Commanding General, Air Research and Development Center Baltimore, Maryland	(1)	WCTSE Engineering Branch, Technical Services Section, Flight Test Division, Hq WADC, WPAFB	(2)
WCRR Air Research, Research Division, Hq WADC, WPAFB	(1)	WCTSI Instrumentation Branch, Technical Services Section, Flight Test Division, Hq WADC, WPAFB	(1)
WCO Commanding General, Wright Air Development Center WPAFB	(1)	WCOL Liaison Section, Plans and Operations Dept. Hq WADC, WPAFB	(1)
WCO Plans and Operations Dept. Hq WADC, WPAFB	(1)	Commanding General, Air Force Flight Test Center Attn: Flight Test Division Edwards Air Force Base Edwards, California	(1)
WCS Weapons Systems Division, Hq WADC, WPAFB	(1)	Deputy Inspector General, Technical Inspection and Flight Safety Research, Norton Air Force Base, Calif.	(1)
WCEOT Operations Office, Weapons Components Division, Hq WADC, WPAFB	(4)	BAGR Bureau of Aeronautics General Representative, WPAFB	(4)
WCOE Engineering Operations Section, Plans & Operations Office, Hq WADC, WPAFB	(1)	MCLANA NACA Liaison Office WPAFB	(1)
WCE Weapons Components Division, Hq WADC, WPAFB	(1)	MCLI USAF Institute of Technology, WPAFB	(1)
WCN Aeronautics Division, Hq. WADC, WPAFB	(1)		

DISTRIBUTION:	<u>No. of Copies</u>	<u>No. of Copies</u>
MCLAFS Deputy Inspector General for Technical Inspection and Flight Safety Research WPAFB	(1)	Royal Aircraft Establishment, Attn: Mr. H. C. Pritchard, Farnborough Hants, England (1)
The Director, Air University Library, Maxwell AFB, Alabama Attn: Requisition No. CR-399B	(1)	WCSWF Fighter Branch Aircraft Section Weapons Systems Division, Hq WADC, WPAFB (1)
ATIAA Aircraft & Propulsion Section, Air Technical Intelligence Center WPAFB	(1)	WCNS Aircraft Laboratory, Aeronautics Division, Hq WADC, WPAFB (2)
CADO	(1)	WCEG Armament Laboratory, Weapons Components Division, Hq WADC, WPAFB (1)
Technical Library, WPAFB	(1)	WCTW All Weather Section Flight Test Division, Hq WADC, WPAFB (3)
Chief, Bureau of Aeronautics, Attn: Technical Information Br., Code TD-4, Room 1W20, Navy Dept., Washington 25, D.C.	(1)	WCTWE Project Officer All Weather Section Flight Test Division Hq WADC, WPAFB (2)
Director, Naval Research Lab. Technical Information Office, Navy Dept. Washington 25, D.C.	(1)	Director, Ames Aeronautical Laboratory, NACA, Moffett Field, Calif. (1)
Commanding Officer, Naval Air Development Station, Johnsville, Pennsylvania	(1)	Bendix Aviation Corporation, Eclipse-Pioneer Division, Teterboro, New Jersey (1)
Sperry Gyroscope Company, Federal Dept. Great Neck, L.I., New York Attn: Mr. R. E. Ellis	(1)	Boeing Airplane Company Seattle, Washington (1)
		Consolidated-Vultee Aircraft Corp. San Diego, Calif. (1)
		Cornell Aeronautical Laboratory, Cornell Research Foundation, Buffalo, New York (1)

DISTRIBUTION:	No. of <u>Copies</u>
Douglas Aircraft Company, Inc. Long Beach, Calif.	(1)
General Electric Company, Aeronautics & Ordnance Systems Dept., Schenectady, New York	(1)
Goodyear Aircraft Corporation, Akron, Ohio	(1)
Hughes Aircraft Company, Culver City, Calif.	(1)
Lockheed Aircraft Corporation, Burbank, Calif.	(1)
McDonnell Aircraft Corporation, St. Louis, Missouri	(1)
Minneapolis-Honeywell Regulator Company, Minneapolis, Minnesota	(1)
North American Aviation, Inc., Los Angeles, Calif.	(1)
Northrop Aircraft, Inc., Hawthorne, Calif.	(1)
Republic Aviation Corporation, Farmingdale, Long Island, New York	(1)
Westinghouse Electric Corporation, Air Armaments Division, Friendship International Airport, Baltimore, Maryland	(1)
Deputy for Development, Air Research and Development Command, Baltimore, Maryland	(1)